

This article was downloaded by:

On: 15 January 2011

Access details: *Access Details: Free Access*

Publisher *Taylor & Francis*

Informa Ltd Registered in England and Wales Registered Number: 1072954 Registered office: Mortimer House, 37-41 Mortimer Street, London W1T 3JH, UK



Chemistry and Ecology

Publication details, including instructions for authors and subscription information:

<http://www.informaworld.com/smpp/title~content=t713455114>

Comparison between remote-sensed data and *in situ* measurements in coastal waters: The taranto sea case

R. Matarrese^a; V. De Pasquale^a; L. Guerriero^a; A. Morea^a; G. Pasquariello^b; G. Umgiesser^c; I. Scroccaro^c; G. Alabiso^d

^a Dipartimento di Fisica, Università di Bari, Bari, Italy ^b CNR-ISSIA, Bari, Italy ^c CNR-ISMAR, Venezia, Italy ^d CNR-IAMC-Sezione Talassografico 'A. Cerruti', Taranto, Italy

To cite this Article Matarrese, R. , De Pasquale, V. , Guerriero, L. , Morea, A. , Pasquariello, G. , Umgiesser, G. , Scroccaro, I. and Alabiso, G.(2004) 'Comparison between remote-sensed data and *in situ* measurements in coastal waters: The taranto sea case', *Chemistry and Ecology*, 20: 3, 225 – 237

To link to this Article: DOI: 10.1080/02757540410001689795

URL: <http://dx.doi.org/10.1080/02757540410001689795>

PLEASE SCROLL DOWN FOR ARTICLE

Full terms and conditions of use: <http://www.informaworld.com/terms-and-conditions-of-access.pdf>

This article may be used for research, teaching and private study purposes. Any substantial or systematic reproduction, re-distribution, re-selling, loan or sub-licensing, systematic supply or distribution in any form to anyone is expressly forbidden.

The publisher does not give any warranty express or implied or make any representation that the contents will be complete or accurate or up to date. The accuracy of any instructions, formulae and drug doses should be independently verified with primary sources. The publisher shall not be liable for any loss, actions, claims, proceedings, demand or costs or damages whatsoever or howsoever caused arising directly or indirectly in connection with or arising out of the use of this material.

COMPARISON BETWEEN REMOTE-SENSED DATA AND *IN SITU* MEASUREMENTS IN COASTAL WATERS: THE TARANTO SEA CASE

R. MATARRESE^{a,*}, V. DE PASQUALE^a, L. GUERRIERO^a, A. MOREA^a,
G. PASQUARIELLO^b, G. UMGIESSER^c, I. SCROCCARO^c and G. ALABISO^d

^aDipartimento di Fisica, Università di Bari, via Amendola 173, 70126 Bari, Italy; ^bCNR-ISSIA,
Via Amendola 122/0, 70126 Bari, Italy; ^cCNR-ISMAR, S. Polo 1364, 30125, Venezia, Italy;
^dCNR-IAMC-Sezione Talassografico 'A. Cerruti', Via Roma 3, 74100, Taranto, Italy

(In final form 18 February 2004)

Monitoring and managing small coastal ecosystems requires a considerable understanding of the temporal dynamics of biophysical factors describing the coastal water systems. For this reason, daily observation from space could be a very efficient tool. The objective of the work described in this paper is to evaluate the contribution of remote sensing to the continuous monitoring of coastal areas. It is well known that in coastal areas, the presence of inorganic suspended sediments and coloured dissolved organic matter can make chlorophyll-concentration measurements from remote sensing difficult. To overcome these difficulties, an alternative approach to the SeaWiFS standard chlorophyll algorithm is presented, based on a semi-analytic model for sea water and on the use of MODIS data as input in a model for atmospheric effects removal. Moreover, land contamination (mixed sea–land pixels) can introduce ambiguities in sea-surface temperature measurements from remote sensing. This paper proposes the use of a hydrodynamic model as a time–space interpolator of *in situ* campaign data, to extensively validate the temperature values extracted from AVHRR sensor. We validated the proposed approach, using experimental field data collected over a two-year campaign in the Taranto Gulf. The results seem to indicate a good agreement between remote-sensed and *in situ* data.

Keywords: Environmental monitoring; Remote sensing; Chlorophyll; Temperature; Finite elements model; Coastal waters

1 INTRODUCTION

Environmental changes are frequently caused by human activity, particularly on coastal zones where roughly 60% of the population live. In general, remote sensing from space can provide an efficient and economical approach for environmental monitoring. However, the monitoring of coastal waters using the existing satellite instruments, optimized for open ocean waters, is a challenging task which requires certain special procedures.

In fact, we know that in open oceans, case 1 waters, phytoplankton is the principal agent responsible for the optical properties of waters. However, the optical properties of shallow coastal waters, case 2 waters, are influenced not only by phytoplankton, but also by other

* Corresponding author. E-mail: raffaella.matarrese@ba.infn.it

substances, generally classified as suspended inorganic particles and yellow substance (Bukata *et al.*, 1995; IOCCG, 2000).

For this reason, there is a need to develop an appropriate algorithm for chlorophyll concentration retrieval from remote-sensing data in coastal areas. Furthermore, the spatial resolution of the ocean sensors, even with the required spectral and temporal resolution, is not entirely suitable in coastal areas of small extension.

In this paper, we compare the values obtained from remote-sensing data for two important physical parameters, the sea-surface temperature and the chlorophyll *a* concentration, with *in situ* measurements of the same parameters in the Taranto Sea area, where ground data are available.

To compare point-like data from *in situ* measurements with space data averaged over the pixel area and taken at different times, we developed a detailed hydrodynamic model of the two basins. For the determination of chlorophyll *a* concentration, we selected only uncontaminated pixels totally covered by water. Then, we compared standard algorithms with a semi-analytic model, which has an appropriate atmospheric correction procedure near the coastal line.

2 MATERIAL AND METHODS

2.1 Study Area

The Taranto Sea represents a coastal marine ecosystem which has been gradually modified by anthropogenic activities. It is situated by the Ionian Sea and is composed of two parts: the Mar Grande and the Mar Piccolo.

The Mar Grande covers an area of 35 km² with a maximum depth of about 35 m and an average depth of about 15 m. It connects with the Ionian Sea through two apertures. The Mar Piccolo of Taranto has a total surface area of 20.72 km² and is composed of two shelves, the 'First Seno' and the 'Second Seno'. The maximum depth is about 15 m for the First Seno and about 10 m for the Second Seno. The Mar Piccolo is characterized by the presence of about 30 submarine freshwater springs and a water pump serving the industrial plant of ILVA that picks up about 35 m³ s⁻¹ from the First Seno of the Mar Piccolo.

Problems due to increasing pollution from various sources are reducing the environmental quality of the Taranto Sea. In fact, it is exposed to industrial pollution and receives a considerable amount of sewage from the northern part of Taranto and from the nearby towns. Several studies have been carried out to characterize the situation, but a modelling approach has not been performed until now (Alabiso *et al.*, 1997, 2000).

2.2 *In Situ* Measurements

In situ measurements used in this work were performed by CNR-IAMC Section of Taranto Talassografico 'A. Cerruti'. Nine fixed stations were monitored with an almost monthly frequency. Figure 1 shows the distribution of measurement sites inside the area.

In each station, the following variables were measured: temperature, salinity and chlorophyll *a* (Chl-*a*). For this work, we made measurements at a depth of 1 m throughout the years 2000 and 2001. During this period, 27 measurements for each station were performed, and all measurements were taken between 9.00 a.m. and 1.00 p.m. local time. Salinity and temperature were measured using a ME CTD 1500 probe. The Mar Grande is a purely marine environment, with salinity values higher than 38 Practical Salinity Units (psu); the Mar Piccolo receives several inputs of freshwater so that the salinity values are always lower than 37 psu, frequently reaching 35 psu. Chl-*a* was extracted in anhydrous methyl alcohol

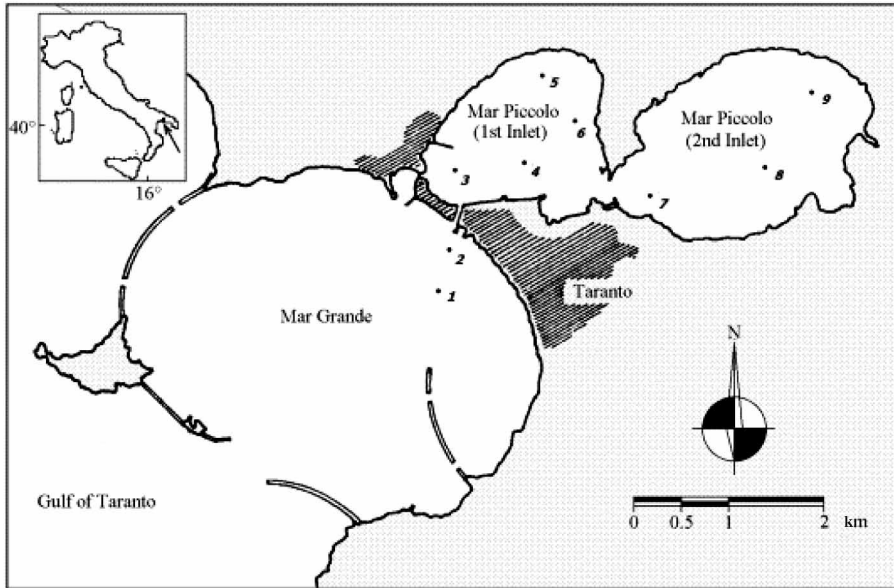


FIGURE 1 Taranto Seas with field stations.

according to Talling and Driver's (1963) method. As we were interested in measuring Chl-*a* in routine sampling on several samples, we used the methanol extraction method instead of the acetone method because it is easier (requires no dilution or neutralization, and absorbance can be read after 4 h; Subba Rao *et al.*, 2002).

2.3 Remote-Sensing Data

AVHRR data were collected daily for the whole of 2000, as an SST map product from the website www.eoweb.de. This product was the first result of DLR's AVHRR pathfinder activities. First, a process of autonavigation was performed using a coastline to improve the accuracy of the georeferentiation. To determine the multi-channel sea-surface temperature (MCSST), a formula based on the brightness temperatures of AVHRR channels 4 (T4) and 5 (T5) was applied, as described by McClain *et al.* (1985). This technique is known as the 'Split Window Technique' and corrects for atmospheric attenuation, mainly caused by absorption of water vapour; this normally leads to a significant drop in the brightness temperatures. The SST values were obtained using the following equation:

$$\begin{aligned} \text{SST} = & A \times T4 + B \times (T4 - T5) + C \times (T4 - T5) \times (\text{SEC}(sza) - 1) \\ & + D \times (\text{SEC}(sza) - 1) + E \end{aligned}$$

where the coefficients A, B, C, D and E depend both on day/night passage and on the AVHRR-specific sensor, and *sza* is the solar zenith angle.

The data were remapped into a standard Mercator projection with geometric resolution at the centre of the satellite map of 1.1132 km. All data were transformed to the fixed grid projection by resampling the dataset on a pixel-by-pixel basis, using a nearest-neighbour algorithm.

SeaWiFS data were acquired by the receiving station, HROM, in Rome. These images have the best geometry of acquisition for the Taranto area. The acquisition time was

around 11.00 a.m., so the period between satellite passage and *in situ* measurements was less than 2 h. This short time difference allowed us to assume that the *in situ* measurements and satellite images were acquired at the same time. From the overall SeaWiFS dataset corresponding to in-field measurements, only cloud-free images were selected. The result of this selection was a set of five images: two images in 2000, both in June (5 and 20 June), and three images in 2001 (14 and 30 May and 26 July).

2.4 Methodology

2.4.1 Hydrodynamic Model of the Taranto Sea

In our dataset, direct comparisons of the sea-temperature truth data with AVHRR SST data were not feasible, as the position of the field stations was too close to the coastal line.

To solve this problem, a bidimensional hydrodynamic model of the Taranto Sea was implemented. The model, developed at ISMAR-CNR, solves the well-known shallow-water equations in the vertically integrated form. The model was also provided with dispersion and heat-flux modules. The numerical computation of the main hydrodynamic unknowns was based on the finite element (FE) method, which is especially suited to shallow-water areas.

A semi-implicit scheme was adopted for the integration in time, while a FE computational method was used for the integration in space of the main system unknowns. Using a combination of linear and constant form functions, the FE method estimates the water velocity and the sea-surface level over the whole basin domain and for the entire simulation.

The model was based on two horizontal, vertically integrated, momentum equations and on a mass-conserving equation, corresponding to the shallow-water equations in the Boussinesq approximation form. In this formulation, the wind and the bottom friction terms were in quadratic form and parameterized. The dispersion and the heat modules were coupled with the hydrodynamic model to preclude any problems of data exchange (Umgiesser *et al.*, 1995; Umgiesser, 1998).

The tides, meteo data (wind, air, temperature, rainfall, etc.) and various inflows into the Taranto Sea were taken into account as force factors. The two inlets of the Mar Grande were considered as open boundary conditions, and the tidal elevation was imposed.

The tidal data were measured using a tide gauge, provided by the Servizi Tecnici Nazionali, situated on the Canale di Porta Napoli along the old Taranto island. Spring tides have a range of about ± 0.15 m and neap tides about ± 0.08 m. The river runoff and wastewater discharge values come from the Biology Department of Bari University. These inflows into the basin were considered as constant values. It should be stressed that considerable seasonal fluctuations may change these values intermittently.

For wind, data were collected from the Istituto Meteorologico 'L. Ferrajolo' of Taranto as wind speed and direction. The station was located along the coast at about 6 km from the city of Taranto. The same station also measured other meteo data, necessary for the dispersion and radiance modelling, such as solar radiation, air temperature, relative humidity and cloud cover. In particular, the solar radiation data were obtained from heliophany data by conversion using an empirical formula (Benincasa *et al.*, 1991).

The simulation was carried out using a time step of 600 s, and the model was allowed to achieve a steady state for 4 months, beginning 1 September 1999. Then, the simulation for the year 2000 started. The hydrodynamic and temperature fields were computed, based on the simulation results.

2.4.2 Chlorophyll Determination in Shallow Waters

Before using the chlorophyll retrieval algorithms, a pre-processing procedure was necessary.

Because of the low extension of the Taranto Sea, special care was taken in selecting SeaWiFS images of pure sea pixels, *i.e.* pixels not contaminated by land patterns. To achieve this goal, a fine geolocation procedure was followed, using the geolocation information contained in the SeaWiFS image file and a coastline of the Taranto marine area acquired from a cartographic map at a scale of 1:100,000. Only the pixels completely contained inside the basins defined by the coastline were selected for further analysis. The pixels' positions and dimensions changed within the image. For the almost nadir images, we had a maximum of 14 pixels in the Mar Grande and two pixels in the Mar Piccolo, while in the off-nadir image, the maximum number of pixels selected was three for the Mar Grande and no pixels in the Mar Piccolo.

A second pre-processing step concerned the atmospheric correction of the pure sea pixels obtained by the previous method. For case 1 waters, the atmospheric correction algorithms are based on the assumption that the values of water-leaving radiance in the near-infrared are negligible (black pixel assumption). For case 2 waters, this assumption is no longer valid (Siegel *et al.*, 2000), and algorithms developed for case 1 fail. Improvements in atmospheric-correction algorithms for case 2 waters have been carried out, replacing the black pixel assumption. For example, according to Hu *et al.* (2000), it was assumed that the type of aerosol is constant for small spatial regions, while according to Ruddick *et al.* (2000), it was proposed that the 765/865 nm ratio for aerosol reflectance and for water-leaving reflectance is spatially homogenous. The authors of the last paper modified the SeaDAS software (<http://seadas.gsfc.nasa.gov>), the standard software for SeaWiFS image processing, to perform calculations which implement the new assumption (SeaDAS Mumm) (<http://www.mumm.ac.be/OceanColour>). In our approach, the atmospheric correction of the images was performed using the code 6s (Vermote *et al.*, 1997). The computer code 6s is a radiative transfer code developed by the Laboratoire d'Optique Atmosphérique in Lille, France. It can be used to correct atmospheric effects on satellite or airborne remote-sensing data to predict the remote-sensing signal between 250 and 4000 nm at the water surface. The code considers several absorbing gasses as well as aerosol effects, provided that the user specifies an aerosol concentration and aerosol composition. The spectral integration is done in steps of 2.5 nm. Input parameters to code are: geometrical conditions, atmospheric model for gaseous components, aerosol model, spectral conditions and ground reflectance. In our case, the geometrical conditions were taken from the SeaWiFS image file. The atmospheric model and the aerosol model were considered constant for the selected pixels due to the low extension of the area. As an atmospheric model, we used the US64 model and took parameters from the MOD09CRS file. These parameters were the total concentration in the air column of the water vapor and ozone. As an aerosol model, we used a bivariate log-normal distribution and took parameters from the MODIS (MOD04) aerosol product file (King *et al.*, 2003). A critical role was played by the aerosol concentration that the 6s computed from an aerosol optical depth at 550 nm: we extracted this information from the MOD04. Concerning the spectral input to 6s code, we used an appropriate filter function for the SeaWiFS bands. Inhomogeneous ground with no directional effects was assumed for the pixels near the coast, while homogeneous ground, with no directional effects was assumed for the other pixels. The 6s output was the ground reflectance; atmospheric effects were removed and a conversion to reflectance was performed. Table I summarizes the atmospheric parameters used as input for 6s code.

Afterwards, the algorithms could be used to determine the chlorophyll concentration from reflectance values. The classical approach, to extract the chlorophyll concentration from reflectance in oceanic waters, is based on empirical models that utilize a band ratio approach considering the spectral features of Chl-a. Two algorithms, named Ocean Color 2 and 4 (OC2 and OC4), developed by NASA use a large dataset of oceanic measurements of chlorophyll

TABLE I Details of some of the atmospheric parameters used in the 6s code.

Day	AOT	H ₂ O (g cm ⁻²)	O ₃ (cm atm)
5/6/2000	0.614	2	0.3275
20/6/2000	0.326	2.06	0.3375
14/5/2001	0.339	1.18	0.375
30/5/2001 (Mar Grande)	0.143	2.08	0.3025
30/5/2001 (Mar Piccolo)	0.156	2.08	0.3025
26/7/2001	0.285	—	—

Note: AOT: aerosol optical thickness. For 26/7/2001, we did not have the MOD09CRS image. We used the standard model Midlatitude Summer for the atmosphere and the Urban Model for the aerosol distribution.

concentration. The number indicates the amount of bands used. These empirical methods do not produce satisfactory results in case 2 waters because the three main active optical substances are not correlated in these waters. For this reason, we preferred to adopt an SA model developed by Garver and Siegel (1997) and optimized by Maritorena *et al.* (2002). The relationship between the normalized water-leaving radiance, which is equivalent to the reflectance, and the inherent optical properties (IOP) are:

$$\hat{L}_{wn}(\lambda) = \frac{tF_0(\lambda)}{n_w^2} \sum_{i=1}^2 g_i \left[\frac{b_b(\lambda)}{b_b(\lambda) + a(\lambda)} \right]^i,$$

where F_0 is the extraterrestrial solar irradiance, t is the sea-air transmission factor, n_w is the real part of the index of refraction of the water, and g_i are constants. The coefficient of absorption $a(\lambda)$ is partitioned in $a(\lambda) = a_w(\lambda) + a_{chl}(\lambda) + a_{cdm}(\lambda)$, while the coefficient of backscattering in $b_b(\lambda) = b_{bw}(\lambda) + b_{bp}(\lambda)$. The suffix ‘w’ refers to the pure water, chl refers to the chlorophyll, and cdm refers to the combined dissolved and particulate matter. The a_{chl} is modelled as $a_{chl}(\lambda) = Chl a_{chl}^*(\lambda)$, where $a_{chl}^*(\lambda)$ is the chlorophyll-specific absorption coefficient, and Chl is the unknown chlorophyll concentration. The $a_{cdm}(\lambda)$ is modelled as $a_{cdm}(\lambda) = a_{cdm}(\lambda_0) \exp[-S(\lambda - \lambda_0)]$, where S is the spectral decay constant; the $b_{bp}(\lambda)$ is modelled as $b_{bp}(\lambda) = b_{bp}(\lambda_0)(\lambda/\lambda_0)^{-\eta}$, where η is the power law exponent. The other unknowns are $a_{cdm}(\lambda_0)$ and $b_{bp}(\lambda_0)$; η was assumed to be constant. The three unknowns (Chl, $a_{cdm}(\lambda_0)$, $b_{bp}(\lambda_0)$) were obtained minimizing the mean square difference between $L_{nw}(\lambda)$ modelled and measured for the band 1–5 of SeaWiFS. The Levenberg–Marquardt non-linear algorithm was used to minimize the merit function.

3 RESULTS

3.1 Remote-Sensed SST Validation

The first step performed was the model calibration: a detailed description of the activity for model tuning as well as the review of model characteristics are reported in Scroccaro *et al.* (2003). The model parameters were refined with the aim of obtaining a good correspondence between *in situ* campaign data and model distribution for temperature and salinity. With the same aim, a simulation was performed for a period of one year, taking into account different forces such as the tide, the meteo data and the freshwater discharges.

In the case of salinity values, the model reproduces sufficiently well, with the temporal and spatial variability of data collected during the field campaign giving a root mean square error of 0.84 psu, corresponding to a relative error of 1.7%.

A second step in refining model parameters has been achieved by adapting the temperature temporal distribution simulated by the model to the *in situ* data. Figure 2 shows the model outputs obtained after this calibration stage. As can be seen, the seasonal behaviour of real data is reproduced well by the model curves, and the agreement between simulated and real data is very good, giving an overall root mean square error of 1.2 °K.

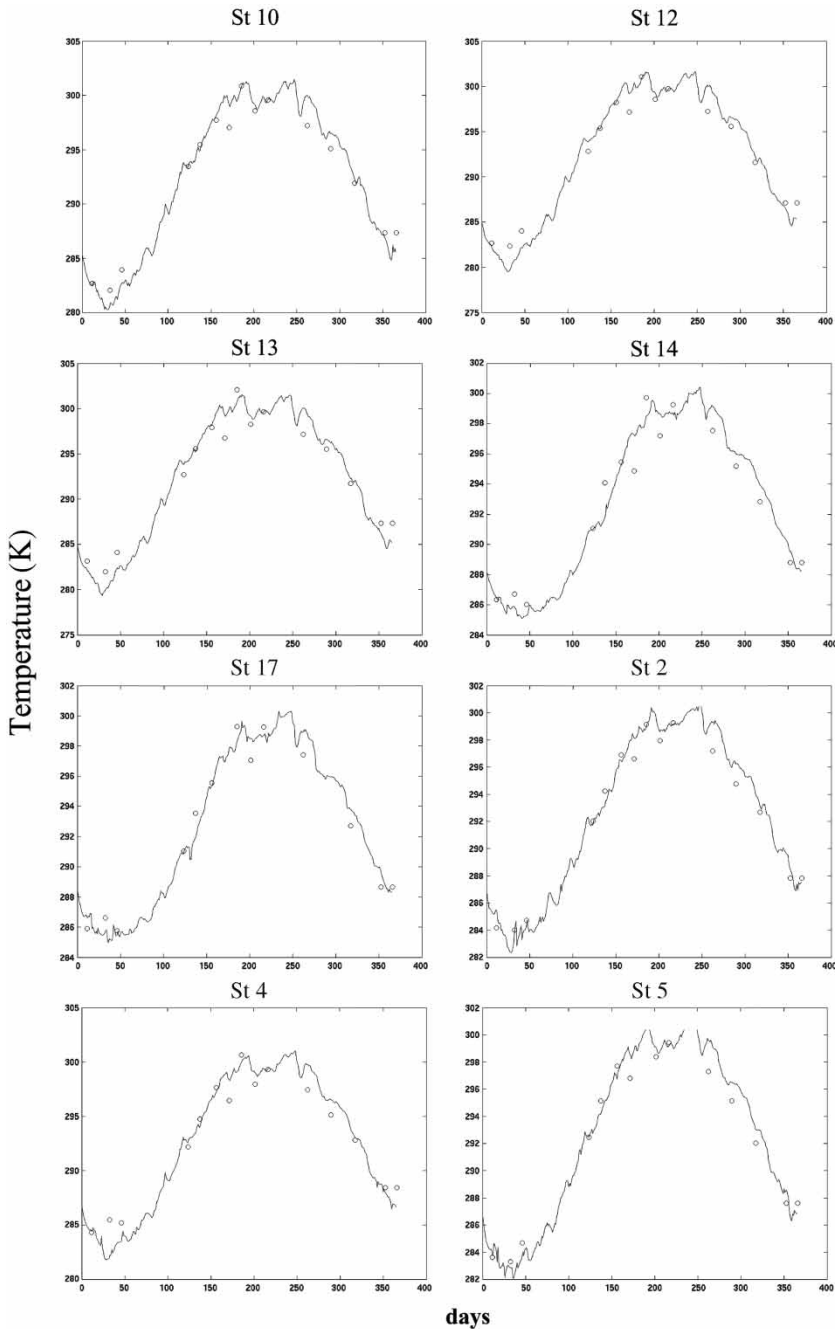


FIGURE 2 Comparison between model results and *in situ* data for the year 2000.

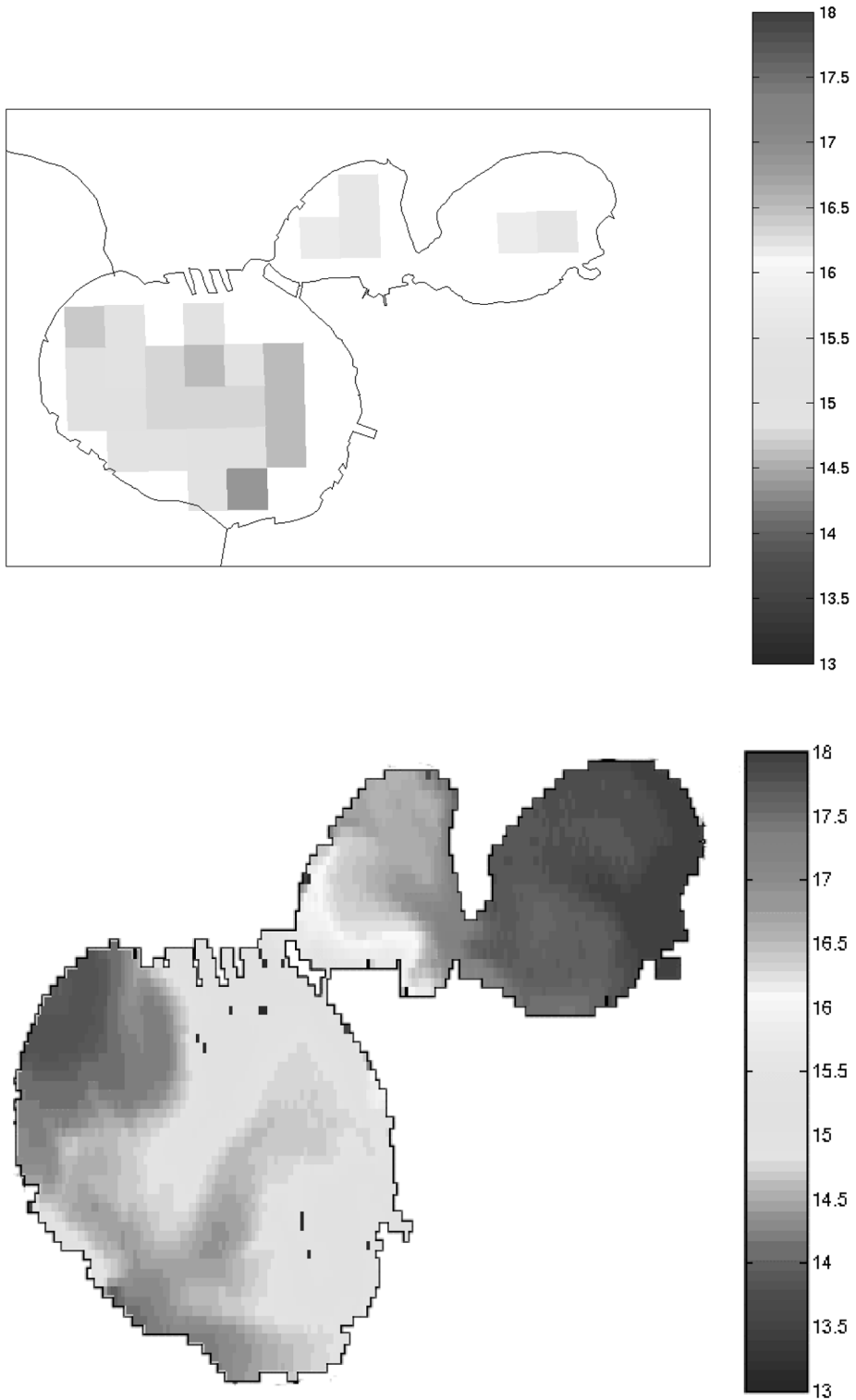


FIGURE 3 Distribution of temperature for 21 April 2000, AVHRR data (top) and model simulation (bottom).

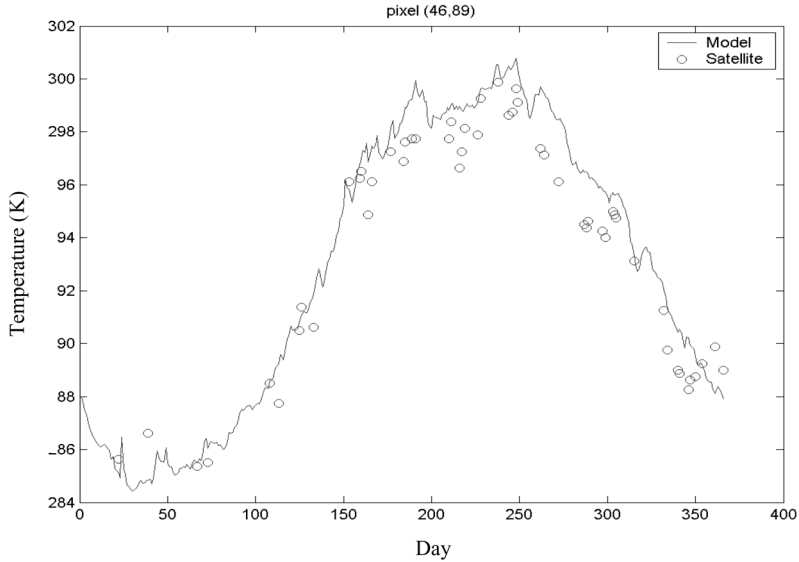


FIGURE 4 Temporal comparison between model results and AVHRR data for the year 2000.

The daily passage of the satellite on the investigated area gives a map of the Taranto Seas reproduced by 42 pixels $1.1 \times 1.1 \text{ km}^2$. A comparison between the RS data and the model results was carried out, considering for each pixel the SST value by AVHRR and the space average modelled temperature value obtained for the corresponding area. Figure 3 shows the highly dynamic behaviour of physical parameters, in this case, temperature. For this reason, dynamical model data were averaged properly for comparison with the low-resolution spatial data from the satellite.

The domain was subdivided into three different areas of investigation: the Mar Grande offshore area with 12 pixels, the Mar Grande inner area with six pixels and the Mar Piccolo area with two pixels. For each case, the RS and the model temperature time series were taken into account.

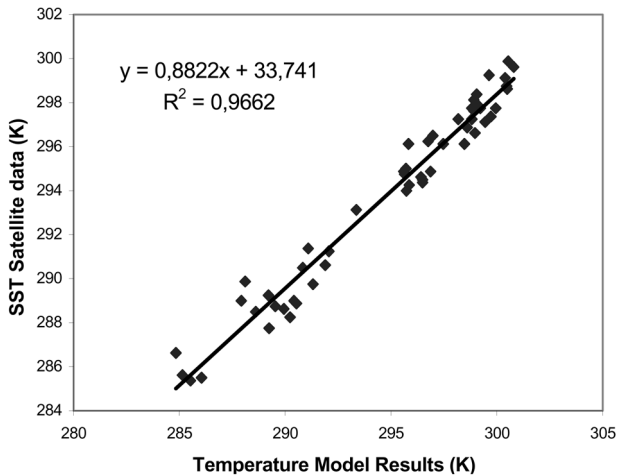


FIGURE 5 Scatterplot of AVHRR vs. model sea surface temperature for the year 2000.

For the first area, the SST data presented an RMS equal to 1.05 K affected by a bias of -0.86 K, with respect to the model results. The correlation index was 0.96 (Figs. 4 and 5). In the second case, the RMS between the two series was 1.18 K, with a bias of -1.18 K. The two series were linearly correlated at the 0.91 value. In the Mar Piccolo area, where only 10 measurements were available for two useful AVHRR pixels, the results showed an average error of 2.5 K, corresponding to 12% error with respect to the 21 K of annual thermal excursion in the same area. This result was the worst among those relative to the three areas, but it provided useful information for such a small basin.

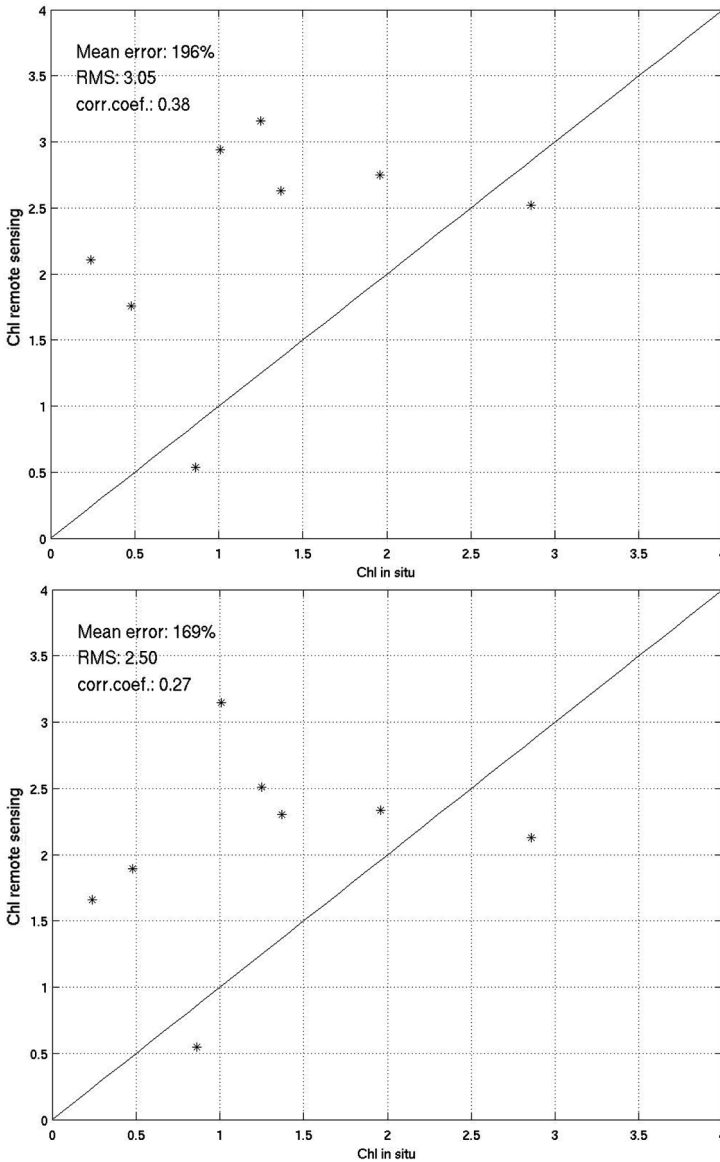


FIGURE 6 Scatterplot of *in situ* measurements and OC2 (top) and OC4 (bottom) ocean colour algorithm for chlorophyll concentration using SeaDAS Mumm.

3.2 Chlorophyll Retrieval

From the selected SeaWiFS images, we extracted 59 useful pixels. For each pixel, we attempted to calculate the chlorophyll concentration using the three procedures described above. Using the NASA ocean colour algorithm OC2 and OC4, performed using SEADAS software, we found no useful pixels in the images for the Taranto marine area because of the failure of the atmospheric correction specific for open clear waters. The atmospheric correction implemented in the SeaDAS Mumm has given better results; in fact, we have found 51 pixels not flagged, for which we have calculated chlorophyll concentration using OC2 and OC4 ocean colour algorithms.

For each ground point, we selected the pure sea pixel covering the area around the ground stations or, in any case, the nearest ones. If more than one SeaWiFS pixel had about the same distance from the ground point, the mean of the corresponding chlorophyll concentration values was taken into account.

With SeaDAS Mumm, we were able to accept eight pixels among those matching the ground measurements. The low number of matching points is due to the fact that seven of the nine stations were situated in the Mar Piccolo, where it was possible to select only a few SeaWiFS pixels, because of the low extension of this basin. Figure 6 shows the results obtained: in this case, the mean percentage error was 196% and 169%, respectively, and the correlation coefficient was 0.38 and 0.27, respectively. It is evident that the empirical approaches for chl estimates give unsatisfactory results for the Taranto marine area.

Performing the atmospheric correction with the 6s code and retrieving the chl concentration with the semi-analytic model to the images, we were able to accept 10 pixels among those matching the ground data. The results are shown in Fig. 7. The mean percentage error found was 33%, with a correlation coefficient of 0.78. The figure shows that the model underestimates the chlorophyll concentration data. This underestimation is probably because the semi-analytic model was optimized for ocean waters, where the range of chlorophyll was narrower than coastal waters.

Figure 8 shows the distribution of chlorophyll concentration, for 5 June 2000, retrieved from SeaWiFS data, using the proposed approach. The highest concentration of chlorophyll

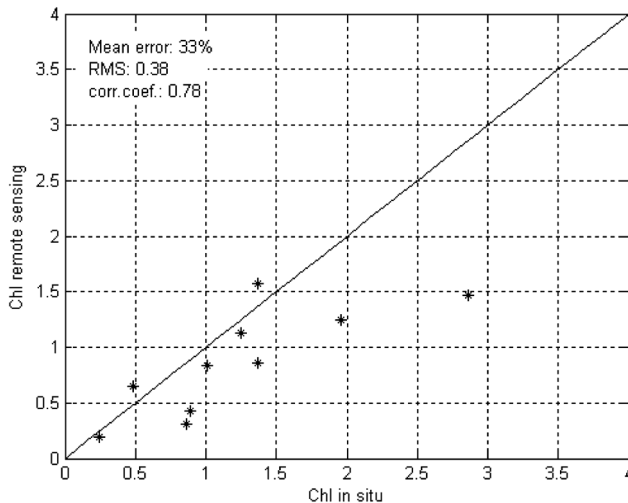


FIGURE 7 Scatterplot of *in situ* measurements and chl concentration obtained from the SeaWiFS image.

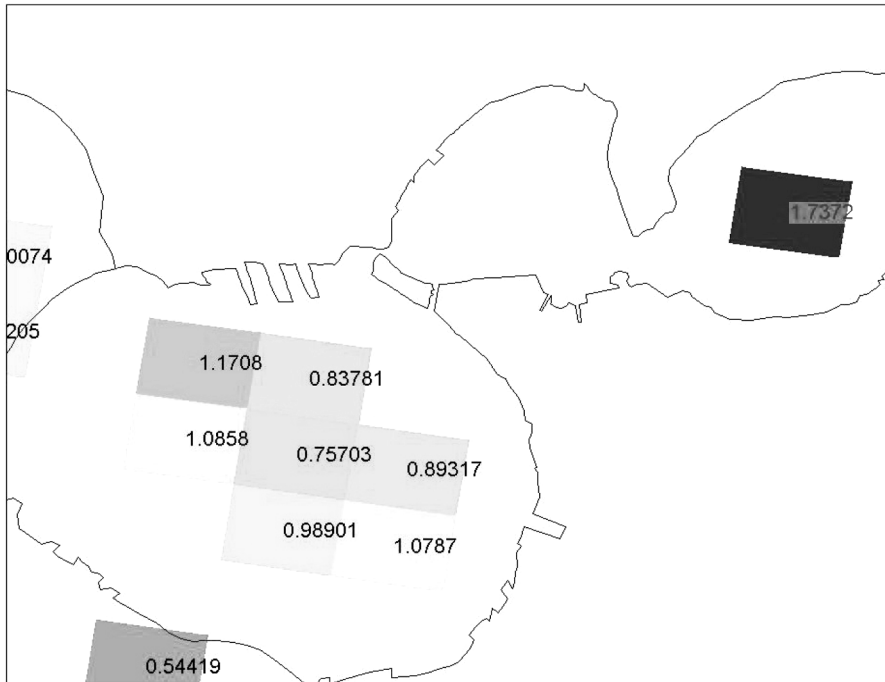


FIGURE 8 Distribution of chlorophyll concentration, 5 June 2000, using SeaWiFS data.

is detected in correspondence of ‘Secondo Seno’ of Mar Piccolo and decreasing values of concentration are showed going from Mar Piccolo to open sea.

4 CONCLUSION

This paper illustrates the application of remote sensing data for the analysis of a small coastal water system. Attention has been focused on extracting two parameters useful for describing the status of the observed ecosystem: sea-surface temperature and chlorophyll concentration.

The hydrodynamic finite element model was useful in validating the remote-sensed sea surface temperature measured by standard algorithms in the coastal water of the Taranto Gulf. In fact, by using this tool, to follow and describe the evolution of the main physical parameters, the few ground control points can be used to calibrate the whole region of interest.

We found a good agreement between the remote-sensed SST and the modelled temperature results over the whole investigated area. Nevertheless, the agreement improves, moving from the near-shore to the offshore areas, with the highest correlation values for the open sea zones. This is clearly due both to the influence of the mixed land–sea pixels and to the use of specific algorithms mainly suitable for the open sea areas analysis.

As far as chlorophyll concentration retrieval is concerned, our results seem to indicate that SeaWiFS data can be usefully exploited also in low extensions and almost closed coastal basins. In fact, the experiment shows that a good correlation between *in situ* measurements and chlorophyll concentration retrieved from SeaWiFS images can be achieved by using an accurate geolocation procedure, atmospheric correction tool and accurate semi-analytic model.

Acknowledgements

This research was carried out by the Physics Department, University of Bari in the framework of SPICAMAR project in Taranto Gulf, supported by CONISMA with the collaboration of ISMAR-CNR of Venice, ISSIA-CNR of Bari, IAMC-CNR of Taranto. The authors thank the reviewers for their constructive and useful comments.

References

- Alabiso, G., Cannalire, M., Ghionda, D., Milillo, M., Leone, G. and Caciorna, O. (1997). Particulate matter and chemical-physical conditions of an inner sea: the Mar Piccolo in Taranto. A new statistical approach. *Marine Chemistry*, **58**, 373–388.
- Alabiso, G., Cannalire, M., Milillo, M., Venturelli, G. and Pacifico, P. (2000). Carbohydrates, proteins and chlorophyll-*a* in the suspended matter of surface waters in The Mar Piccolo of Taranto (Gulf of Taranto, Ionian Sea). *Atti del XXX cong. società Italiana di biologia marina*. Vibo Valentia 7-12 Giugno 1999. *Biologia Marina Mediterranea*, **7**, 874–880.
- Benincasa, F., Maracchi, G. and Rossi, P. (1991). *Agrometeorologia*. Pàtron Editore, Bologna.
- Bukata, R. P., Jerome, J. H., Kondratyev, K. Y. and Pozdnyakov, D. V. (1995). *Optical Properties and Remote Sensing of Inland Sand Coastal Waters*. CRC Press, Boca Raton, FL.
- Garver, S. A. and Siegel, D. A. (1997). Inherent optical property inversion of ocean color spectra and its biogeochemical interpretation. I. Time series from Sargasso Sea. *Journal of Geophysical Research*, **102**, 18607–18625.
- Hu, C., Carder, K. L. and Muller-Karger, E. (2000). Atmospheric correction of SeaWiFS imagery over turbid coastal waters: a practical method. *Remote Sensing of Environment*, **74**, 195–206.
- IOCCG Report Number 3 (2000). Remote sensing of ocean color coastal, and other optically-complex, water [<http://www.ioccg.org/reports/report3.pdf>].
- King, M. D., Menzel, W. P., Kaufman, Y. J., Tanre, D., Gao, B. C., Platnick, S., Ackerman, S. A., Remer, L. A., Pincus, R. and Hubanks, P. A. (2003). Cloud and aerosol properties, precipitable water, and profiles of temperature and water vapor from MODIS. *IEEE Transactions on Geoscience and Remote Sensing*, **41**, 442–458.
- Maritonera, S., Siegel, D. and Peterson, A. (2002). Optimization of a semianalytical ocean color model for global-scale application. *Applied Optics*, **41**, 2705–2714.
- McClain, E. P., Pichel, W. G. and Walton, C. C. (1985). Comparative performance of AVHRR based multichannel sea surface temperature. *Journal of Geophysical Research*, **90**, 11587–11601.
- Ruddick, K. G., Ovidio, F. and Rijkeboer, M. (2000). Atmospheric correction of SeaWiFS imagery for coastal and inland waters. *Applied Optics*, **39**, 897–912.
- Scroccaro, I., Matarrese, R. and Umgiesser, G. Application of a finite element model to the Taranto Sea. *Chemistry and Ecology*. (in press).
- Siegel, D. A., Wang, M., Maritonera, S. and Robinson, W. (2000). Atmospheric correction of satellite ocean color imagery: the black pixel assumption. *Applied Optics*, **39**, 3582–3591.
- Subba Rao, D. V. (2002). Determination of phytoplankton pigments, in Subba Rao, D. V. (ed.) *Pelagic Ecology Methodology*. Balkema, pp. 113–120.
- Talling, J. F. and Driver, D. (1963). Some problems on the estimation of chlorophyll-*a* in phytoplankton. US Atomic Energy Comm., in *Proceedings of Conference of Primary Measurements, Marine and Freshwater, Hawaii TID 7633*, pp. 142–146.
- Umgiesser, G. and Bergamasco, A. (1995). Outline of a primitive equations finite element model, in *Rapporto e studi*, Istituto Veneto of Scienze, Lettere e Arti, Venice, Vol. XII, pp. 291–320.
- Vermote, E., Tanrè, D., Deuzè, J. L., Herman, M. and Morcrette, J. J. (1997). Second simulation of the satellite signal in the solar spectrum, in *User Manual Version 2*. University of Maryland/Laboratoire d'optique Atmosphérique. [http://www.cs.sun.ac.za/~caz/6S/6Smanv2.0_P1.pdf].